WCTE 2014 Quebec City Canada August 10-14
World Conference on Timber Engineering

EQUIVALENT VISCOUS DAMPING FOR CLT INFILLED STEEL MOMENT FRAME STRUCTURES

Matiyas Ayalew Bezabeh[1], Solomon Tesfamariam[2], Siegfried F. Stiemer[3]

ABSTRACT: In the direct displacement based design method, energy dissipative capacity of structures can be represented by an equivalent viscous damping (EVD). A number of studies have been reported in the formulation of EVD for different structural systems and hysteretic models. In this paper, an EVD model is developed for steel-timber hybrid structure, where Cross Laminated Timber (CLT) shear panels are used as an infill in steel moment resisting frames. To develop the EVD model, 243 single-storey single-bay CLT in-filled SMRFs models are developed and subject to cyclic analysis. Different engineering parameters are varied: gap between CLT panel and steel frame, bracket (connection) spacing, CLT panel thickness and strength, and post stiffness yield ratio of steel members. The EVD and ductility of each model were calculated from the hysteretic responses. Design of computer experiments and response surface methodology were utilized to formulate the desired relationship between coefficients of EVD-ductility law and modeling parameters. As a result, an expression is presented to compute EVD as a function of ductility and various modeling parameters.

KEYWORDS: Cross laminated timber, direct displacement based design, equivalent viscous damping, steel moment resisting frames

1 INTRODUCTION

Generally, displacements due to seismic excitations are related to the damage sustained in the structures and the associated failure [1, 2, 3, and 4]. One of the current major advancement in earthquake and structural engineering is to consider structural deformations as a main input for the deign process [5]. These methods are specifically known as direct displacement based seismic design. Direct Displacement Based Design (DDBD) utilizes a virtual representation of the nonlinear structures with an equivalent linear system through secant stiffness (K_e) and equivalent viscous damping (ξ_{eq}) at peak displacement (Δ_d) as illustrated in Figure 1. This method uses equivalent viscous damping (EVD) to represent the energy dissipative capacity of the structural system. As shown in Figure 1d, the target displacement used to obtain the effective period of structure for the given level of EVD. From this step, the design base shear can be calculated from effective mass (m), secant stiffness (K_e), effective period (T_{eff}), and target displacement (Δ_d) [5].

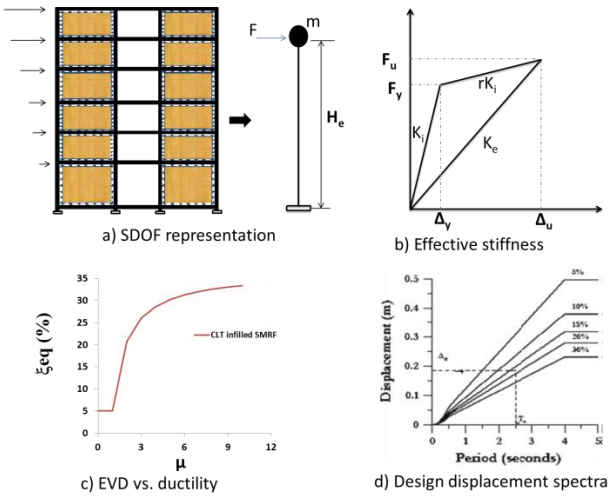

Figure 1: *Basics of DDBD approach* [5]

The EVD concept was introduced by Jacobsen [6], which is based on the idea that nonlinear systems and equivalent linear system under sinusoidal excitation dissipate an equal

[1] M.A.Sc. student, School of Engineering, University of British Columbia, 3333 University Way, Kelowna, BC, Canada, V1V 1V7, Tel: (250)-808-3864, E-mail: mati.aya77@gmail.com
[2] Associate Professor, School of Engineering, University of British Columbia, 3333 University Way, Kelowna, BC, Canada, V1V 1V7, Tel: (250)-807-8185, E-mail: Solomon.Tesfamariam@ubc.ca
[3] Professor, Dept. of Civil Engineering, University of British Columbia, Tel: (604) 822-6301, E-mail: sigi@civil.ubc.ca

amount of energy per cycle of response (Figure 2). The approach proposed by Jacobsen is called the area based approach and shown in Equation 1.

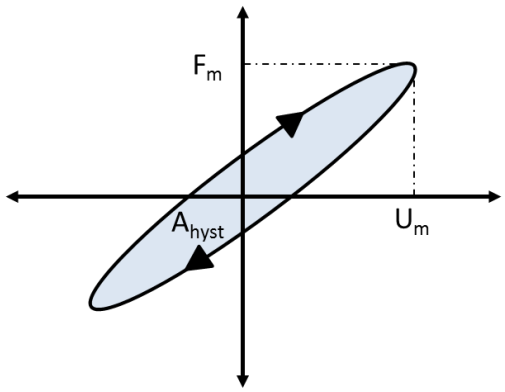

Figure 2: *Hysteretic response area of one cycle*

$$\xi_{hyst} = \frac{1}{2\pi}\frac{A_{hyst}}{F_m U_m} \quad (1)$$

$$\xi_{eq} = \xi_o + \xi_{hyst} \quad (2)$$

where A_{hyst} is the value of dissipated energy; F_m and U_m, respectively, are the maximum force and displacement for the loop (Figure 2). The equivalent viscous damping (ξ_{eq}) in Equation 2 is the summation of elastic damping (ξ_o) and hysteretic component of damping (ξ_{hyst}) [5]. Rosenblueth and Herrera [7] developed the EVD expression based on the secant stiffness. Priestley [8] adopted this for the DDBD method of structures. Miranda and Ruiz-Garcia [9] validated Jacobsen's approach with the secant stiffness to determine inelastic displacement demand of Single Degree of Freedom System (SDOF) system. A comprehensive investigation of the accuracy of Jacobsen's approach was performed by Dwairi and Kowalsky [10] for the Takeda hysteresis model using 100 earthquake records. Kowalsky and Ayers [11] found that the equivalent linear system based on Jacobsen's approach, using effective period at maximum response, yields a good result for the assessment of a non-linear response. Blandon and Priestly [12] compared the EVD based on Jacobsen's approach and EVD from the iterative time history analyses for six different hysteretic models. They concluded that the Jacobson's approach overestimate EVD values and proposed the corrected equations for DDBD method. Recently, the EVD was investigated for different types of structural systems [13, 14, 15, and 16]. Dwairi et al. [13] proposed a hyperbolic damping-ductility law based on nonlinear ductility at a peak displacement as follows:

$$\xi_{\text{hyst}} = \frac{C}{\pi}\left(\frac{\mu - 1}{\mu}\right) \quad (3)$$

where C is a constant, and μ is a ductility ratio. The authors have proposed values of C for unbonded post tensioned concrete systems, reinforced concrete beams, reinforced concrete walls and steel members in terms of the effective period. Wijesundara et al. [14] derived the EVD expression for a concentrically braced frame based on Jacobsen's method and recalibrated the expressions using iterative time history analysis. They have also highlighted that pinching significantly affects the EVD. Ghaffarzadeh et al. [15] proposed new EVD equations for the reinforced concrete (RC) moment resisting frames and RC concentrically braced frames. Lu and Silva [16] estimated EVD for seismic and blast loads for individual and multiple RC members. However, the EVD expression is not yet developed for the timber-steel hybrid system.

The steel-timber hybrid system proposed here, CLT is used as an infill panel in steel moment resisting frames. Since there is no clear hysteresis law to represent the response of the proposed hybrid system, 243 single storey-single bay hybrid systems are analytically investigated to compute EVD based on Jacobson's area based approach and ductility. Different parameters are varied: gap between CLT panel and steel frame, bracket (connection) spacing, CLT panel thickness and strength, and post stiffness yield ratio of steel members. A least square regression method used is to calculate the value of C (Equation 3) for each system. An expression for coefficient C as a function of different parameters are developed using design of computer experiment with response surface method. Finally, the EVD-ductility law is established for the proposed hybrid structure.

2 METHODOLOGY

The method followed to formulate the EVD for the hybrid system is outlined below. A conceptual representation of the hybrid system is shown in Figure 3. Single-storey single-bay frame with the following model variables are considered:

- Three levels of bracket spacing were considered (A): 0.4 m, 0.8 m, and 1.6 m.
- Gap magnitude between steel frame and CLT infill (B) of {20, 50, and 80 mm}, panel thickness (C) of {99, 169, 239 mm}, panel strength (D) of {17.5, 25 and 37.5 MPa}, and post stiffness yielding ratio (E) of {1, 3, 5 %} were selected.

The structural frame elements have been modeled using combination of linear and nonlinear elements. Linear elastic and non-linear displacement based beam-column elements used for the centre and end of the frame member respectively are shown in Figure 3. Modified Ibarra Krawinkler Deterioration model [17] used with a bilinear material property based on moment-curvature relationships is given in the ASCE 41 [18] for nonlinear parts of the frame elements. The section of CLT panel was modeled as

single layer with linear elastic- isotropic wood material property of Quad elements.

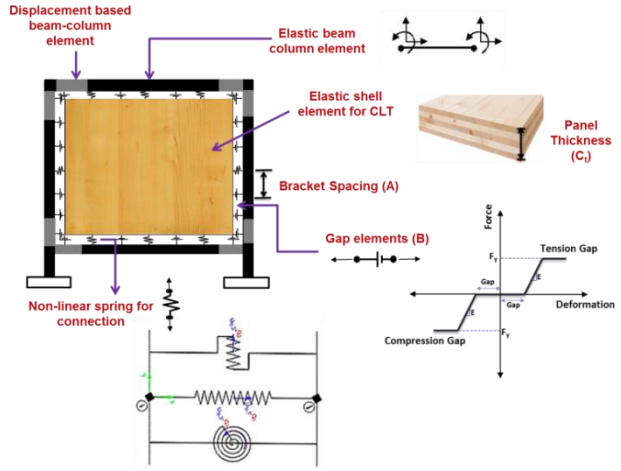

Figure 3: *Details of connection, Gap and CLT infill panels*

The CLT mechanical properties used for modeling can be found elsewhere [19]. The connection between the steel frames and CLT walls was achieved by steel brackets; which were bolted with steel and nailed to CLT panels. The connections are modelled as a spring element using OpenSees's Pinching4 material model calibrated by [20]. Non-linear spring model was used to represent the behaviour of the bracket that connects CLT with steel frame. The bracket behaviour was assigned both in the shear and axial direction. Additionally, the Elastic Perfectly Plastic Gap (EPPG) gap property was modeled in parallel formulation with the axial behaviour of bracket.
Once the analytical models are developed, monotonic static pushover and semi-static cyclic loading analysis are carried out. The parameters considered in this study are summarized in Table 1. The total combination of all parameters constitutes the 243 models considered.

Table 1: *Modeling variables*

A: Bracket Spacing (m)	B: Gap (mm)	C_t: Panel thickness (mm)	D: Panel Strength (MPa)	E: Post Yield Stiffness (%)
0.4	20	99	17.5	1
0.8	50	169	25	3
1.6	80	239	37.5	5

The results of the pushover analysis are used to calculate the yielding and ultimate displacements for each system. Subsequently, the EVD and ductility of each system are computed from the hysteretic responses. Finally, design of computer experiment and response surface method is applied to formulate the damping-ductility law.

3 PARAMETRIC STUDY

3.1 MONOTONIC PUSHOVER ANALYSIS

Static monotonic pushover analysis was carried out for the 243 models. Results of the pushover analysis are used to calculate the yield and ultimate displacement of the system (Figure 4). The yield point of the hybrid system is established based on the displacement corresponding to the smaller of the crushing of panel and yielding of steel. Samples from the results of monotonic pushover analysis are depicted in Figure 4. As shown from the diagram, models having thicker and stronger CLT panels with larger post yield stiffness ratio possess larger load carrying capacity.

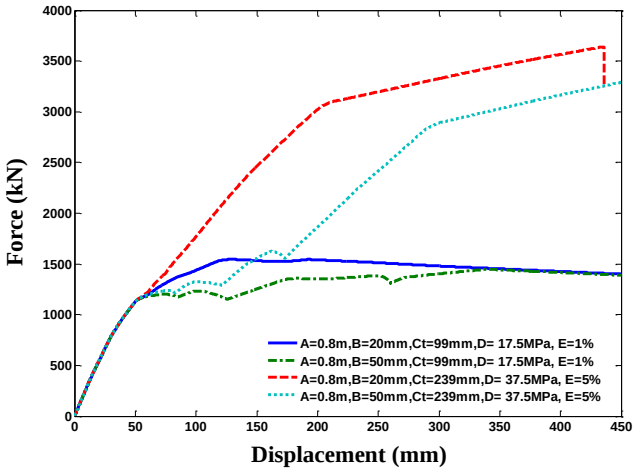

Figure 4: *Capacity curves from monotonic pushover analysis*

3.2 SEMI-STATIC CYCLIC ANAYSIS

A hysteretic response of base shear with lateral displacement is obtained by applying a cyclic displacement history at the top node of each model. The cyclic loading test is conducted according to the CUREE-Caltech Wood frame project protocol [21] (Figure 5). The ultimate displacement obtained from the monotonic pushover analysis is used for cyclic test with a correction factor of 0.4 to account for the difference in deformation capacity between monotonic test and cyclic test [21].

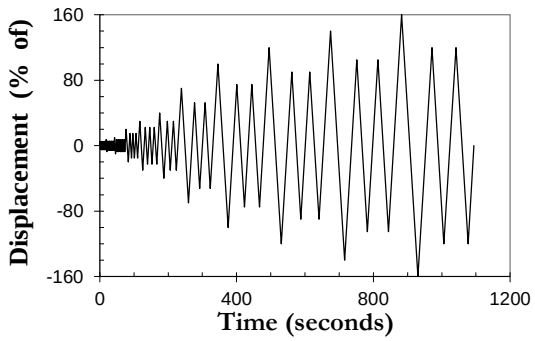

Figure 5: *Cyclic Loading Protocol CUREE*

Samples from the results of semi-static cyclic analysis are depicted in Figure 6. The responses shown in Figure 6a and 6b are characterised by fat hysteresis loops with large amount of energy dissipation. Also from Figures 6a and 6b, it is clear that the thinner and weaker panels show less pinching behaviour. However, models with thicker and stronger panels with higher post yielding stiffness ratio are characterised by a higher degree of pinching (Figures 6c and 6d). This pinching causes significant reduction in energy dissipation, which creates thinner hysteretic loops.

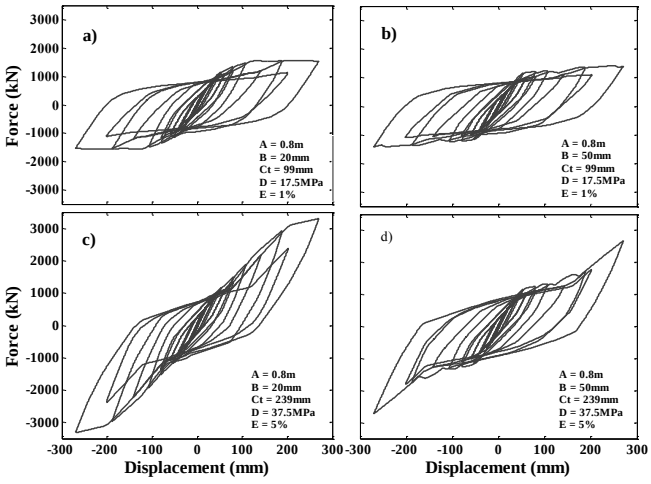

Figure 6: *Hysteretic responses for SDOF model*

4 EQUIVALENT VISCOUS DAMPING

The hysteretic damping corresponding to the cyclic response is calculated for each model based on Equation 1. Then a least square regression was applied to calculate the value of C for Equation 3 from hysteretic damping and ductility values.

Response surface methodology (RSM) with the D-Optimal computer experimental design technique was used to develop an expression for C using the results from least square regression analysis. A second degree polynomial of the form shown in Equation (4) was used to set up relationship between C and the modeling variables (A, B, C_t, D, and E); In Equation 4, C is a regression function, and β0, βi and βij are the regression coefficients.

$$\mathrm{C} = \beta_0 + \sum_{i=1}^{n} \beta_i x_i + \sum_{i=1}^{n} \beta_{ii} x_i^2 + \sum_{i=1}^{n} \sum_{j=1}^{i} \beta_{ij} x_i x_j \qquad (4)$$

In order to develop the desired relationship, data points are selected on the basis of optimality criteria, which are based on the proximity of the predicted response C to the mean response. In order to obtain the coefficients for the proposed second degree equation, 80% of the data points from the least square regression analysis were used for the model training, while the rest were kept aside for statistical validation.

After obtaining significant factors and interactions from RSM, the final expression for C, given in Equation 5, is developed using modeling paramerts of Table 1.

$$C = \Big(0.43 + 0.5 * A + 0.015 * B + (1.27 * 10^{-3} C_t) + (3.75 * 10^{-4} * D) - 0.054 * E - (2.74 * 10^{-4} A * C_t) - (1.01 * 10^{-3} A * D) - 0.019 * A * E + (2.62 * 10^{-5} * B * D) - (3.2 * 10^{-4} * C_t * D) - 0.135 * A^2 - (1.045 * 10^{-4} * B^2) - \left(1.98 * 10^{-6} * {C_t}^2\right) + (5.9 * 10^{-3} * E^2)\Big) \qquad (5)$$

It can be inferred from the Equation 5 that the value of C dependent on the complex interaction between the gap, panel properties and post yielding stiffness ratio of steel frames. The effect of variable interactions is illustrated using response surface plot in Figure 7. These plots were constructed for the indicated axis labels while keeping the other parameters at their median value.

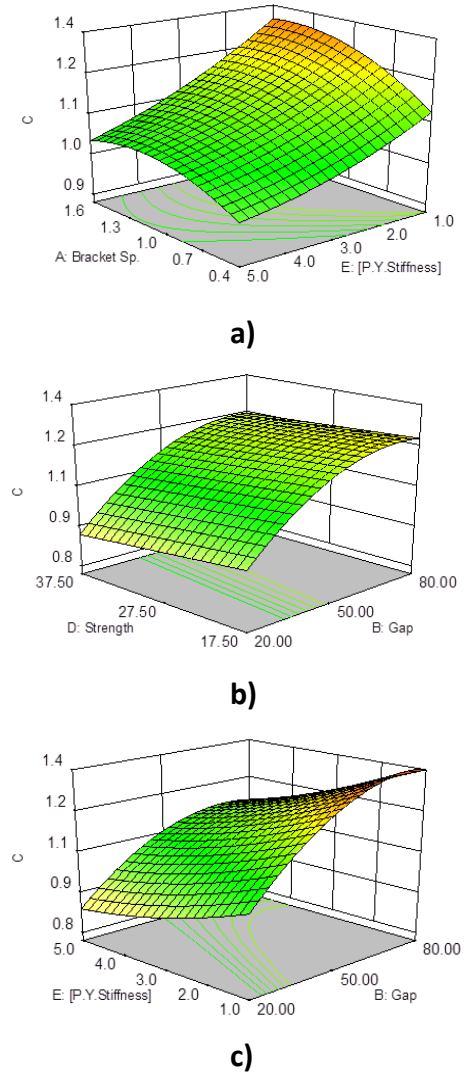

Figure 7: *Response surface plot for the effect of interactions between; a) bracket spacing and post yielding stiffness ratio, b) Panel strength and Gap c) post stiffness yielding ratio and Gap*

Figure 7a shows a decrease in the value of C with an increase in the post the yield stiffness ratio. As discussed

earlier, the higher degree of pinching for systems with a large post yield stiffness ratio prohibits the formation of fat hysteresis loops that in turn decreases the value of C. Moreover, in Figure 7a, for the hybrid systems with larger bracket spacing, the value of C showed an increase in a linear fashion. It is also clear from Figure 7b that the value C is heavily influenced by increasing the magnitude of the gap between CLT panel and steel frame. Originally, the gap was provided to accommodate construction tolerances and to develop the hysteretic behavior. The increase in the gap allows the connection to deform and dissipate energy that increases the value of C. Equation 5 is statically validated for 43 data points outside of the training data set. R2 value of 0.97 was obtained for the plot of actual vs. predicted values of C, as shown in Figure 8.

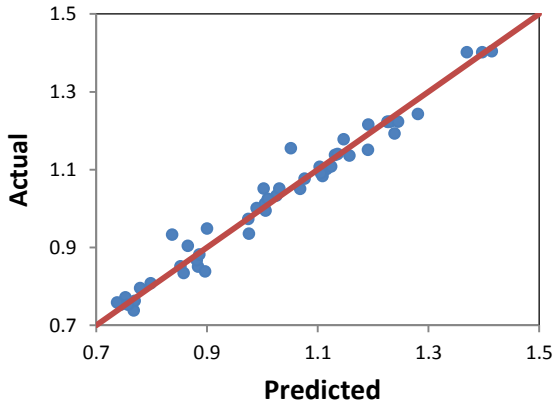

Figure 8: *Validation plot; Predicted vs. Actual (blue/black dots)*

Figure 9 compares the results obtained using the new expression of C (Equation 3 and 5) with the results obtained from other notable studies. In general, the current study obtained the maximum value of ξ_{hyst} in the range of 18%-37% for a ductility value of 10. Referring to Figure 9, results of the proposed equation are between the damping-ductility law given by [22] for bare steel frame and [14] for the concentrically braced steel frames. The damping-ductility law given by [13], for a steel member, is larger than the EVD of the current study. The damping-ductility law suggested by [23] for reinforced concrete frames with masonry infill is similar to the highly pinched models of the proposed hybrid system. In general, the proposed equation proved to be in agreement with rules developed for frames with infill wall and bracings.

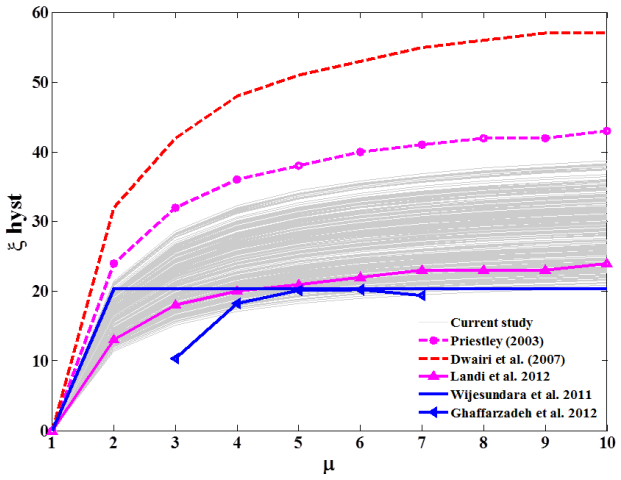

Figure 9: *Comparison of EVD expressions with different researches*

5 CONCLUSIONS

This study proposes an expression for the equivalent viscous damping for CLT infilled Steel Moment Frames. For this purpose, an analytical investigation was carried out for 243 predetermined single-storey single-bay CLT infilled SMRFs by varying the modelling parameters that affect the hysteretic behaviour of the system. The equivalent viscous damping and ductility of each predetermined model obtained from the hysteretic responses of semi-static cyclic analysis. Finally, an expression is developed for equivalent viscous damping as a function of ductility and various modeling parameters. Based on the extensive parametric and statistical tests of the earlier sections, the following concluding remarks can be made:

1. The coefficient C of damping ductility law of Equation 3 is expressed as function of modeling variables of CLT infilled steel moment frames.
2. In general, the hysteretic damping is found to be higher for the hybrid system modeled with larger gap and bracket spacing. Hybrid systems with smaller gap between CLT and steel with larger post yielding stiffness ratio experienced higher degree of pinching. The pinching effect caused the systems to dissipate less amount of energy under cyclic loading.
3. The effect of panel strength and thickness on damping is found to be minimal. This suggests that changing the thickness and crushing strength of panels has little influence on the hysteretic behaviour of the system.

4. Hybrid systems with larger post yielding stiffness ratio dissipate less amount of energy which results lower value of hysteretic damping.
5. From the comparison graphs of Figure 9, it is concluded that for a given level of gap, post yielding stiffness ratio, panel thickness and strength, and bracket spacing, the hysteretic damping is increased linearly up to ductility value of 2.
6. In general, the proposed equation showed to be in a good agreement with laws developed for the frames by other researchers with infill wall and bracings.

ACKNOWLEDGEMENT

This research was supported through funding to the NSERC Strategic Network on Innovative Wood Products and Building Systems (NEWBuildS).

REFERENCES

[1] H. Krawinkler, R. Medina, and B. Alavi: Seismic drift and ductility demands and their dependence on ground motions. *Engineering Structures.*, 25(5):637–653, 2003.

[2] R. A. Medina and H. Krawinkler, Evaluation of drift demands for the seismic performance assessment of frames: *Journal of Structural Engineering.*, 131(7):1003–1013, 2005.

[3] A. Ghobarah, H. Abou-Elfath, and A.Biddah: Response-based damage assessment of structures. *Earthquake Engineering and Structural Dynamics.*, 104:79–104, 1999.

[4] H. S. Kim and Y.S. Chun: Structural damage assessment of building structures using dynamic experimental data. *The Structural Design of Tall and Special Buildings.*, 13(1):1–8, 2004.

[5] M. Priestley, G. Calvi, and M. Kowalsky: Direct displacement-based seismic design of structures. In: *5th NZSEE Conf.*, 1–23, 2007.

[6] L. Jacobsen: Damping in composite structures. In: *Proceedings of the 2nd world conference on on earthquake engineering*, 2: 1029–1044, 1960.

[7] E. Rosenblueth and I. Herrera: On a kind of hysteretic damping. *Journal of Engineering Mechanics Division ASCE*, 1964.

[8] M. Priestley: Myths and fallacies in earthquake engineering-conflicts between design and reality. *New Zealand National Society for Earthquake Engineering.*, 1993.

[9] E. Miranda and J. Ruiz-Garcia: Evaluation of approximate methods to estimate maximum inelastic displacement demands. *Earthquake Engineering and Structural Dynamics.*, 31:3, 539–560, 2002.

[10] H. Dwairi and M. Kowalsky: Investigation of Jacobsen's equivalent viscous damping approach as applied to displacement-based seismic design, *13th World Conference on Earthquake Engineering*,228, 2004.

[11] M. Kowalsky and J. Ayers: Investigation of equivalent viscous damping for direct displacement-based design. In: *The Third U.S.-Japan Workshop on performance-Based Earthquake Engineering Methodology for Reinforced Concrete Building Structures.*, Seattle, W.A, August 2001.

[12] C. A. Blandon and M. J. N. Priestley: Equivalent viscous damping equations for direct displacement based design, *Journal of Earthquake Engineering*, 9(sup2): 257–278, 2005.

[13] H. M. Dwairi, M. J. Kowalsky, and J. M. Nau: Equivalent damping in support of direct displacement-based design, *Journal of Earthquake Engineering*,11(4): 512–530, 2007.

[14] K. Wijesundara, R. Nascimbene, and T. Sullivan: Equivalent viscous damping for steel concentrically braced frame structures. *Bulletin of Earthquake Engineering.*,9(5),1535–1558, 2011.

[15] H. Ghaffarzadeh, A. Jafari, and N. Talebian: Equivalent viscous damping in direct displacement-based design of steel braced reinforced concrete frames. *The Strucural Design of Tall and Special Builidngs*, 2012.

[16] B. Lu and P. F. Silva: Estimating equivalent viscous damping ratio for RC members under seismic and blast loadings, *Mechancis of Research Communication*, 33(6),787–795, 2006.

[17] D. G. Lignos and H. Krawinkler: Deterioration modeling of steel components in support of collapse prediction of steel moment frames under earthquake loading. *Journal of Structural Engineeing*, 137(11): 1291–1302, 2011.

[18] ASCE 41, Seismic rehabilitation of existing buildings. Reston, VA, 2006.

[19] C. Dickof, S. F. Stiemer, M. A. Bezabeh, and S. Tesfamariam: CLT-steel hybrid system: ductility and overstrength values based on static pushover analysis. *Journal of Performance of Constructed Facilities.*, Apr. 2014.

[20] Y. Shen, J. Schneider, S. Tesfamariam, S. F. Stiemer, and Z. Mu :Hysteresis behavior of bracket connection in cross-laminated-timber shear walls, *Construction and Building Materials*, 48,980-991, 2013.

[21] H. Krawinkler, F. Parisi, L. Ibarra, A. Ayoub, and R. Medina: Development of a testing protocol for woodframe structures, Stanford University, 2001.

[22] M. Priestley: Myths and fallacies in earthquake engineering, revisited. In: *The Ninth Mallet Milne Lecture*, 2003

[23] L. Landi, P. Diotallevi, and A. Tardini: Equivalent viscous damping for the displacement-based seismic assessment of Infilled RC Frames, *In: The 15th World Conference on Earthquake engineering*, 2012.